energy&fuels

pubs.acs.org/EF Article

CO_2 Absorption Performance and Electrical Properties of 2-Amino-2-methyl-1-propanol Compared to Monoethanolamine Solutions as Primary Amine-Based Absorbents

Sang-Jun Han and Jung-Ho Wee*

Cite This: *Energy Fuels* 2021, 35, 3197−3207 Read Online

ACCESS | Metrics & More | Article Recommendations

ABSTRACT: Two CO_2 chemical absorption systems using 2-amino-2-methyl-1-propanol (AMP) and monoethanolamine (MEA) aqueous solutions are qualitatively compared in terms of absorption performance and electrical properties. While the absorption capacity is close to their theoretical values in the solutions of concentrations less than 2.0 M AMP and 0.4 M MEA, it decreases below the theoretical values according to the initial concentration (C_{ini}) in the AMP solutions above 2.0 M, and the primary reaction is changed in the MEA solutions above 0.4 M. Unlike the MEA system, the absorption completion time increases proportionally to C_{ini} in the AMP system to be about 247.4 min at the 4.0 M solution; however, the variation of the overall absorption rate of CO_2 follows a parabolic function of C_{ini} with a maximum of 17.98 mmol CO_2/(L·min) in the 0.5 M solution. This difference is primarily due to the instability of AMP carbamate ($AMPCOO^-$) caused by the steric hindrance effects and the inhibition of the $MEACOO^-$ hydrolysis in the two relatively high-concentration solutions. Especially, the amount of generated free-AMP is reduced by the combination of the protonated AMP ($AMPH^+$) generated with $AMPCOO^-$ in the high-concentration solutions. The ionic conductivity of $AMPH^+$ is 29.1 S·cm^2/(mol·z), which is 53.2% less than that of $MEAH^+$, and the real ionic activity coefficient (RIAC) in the AMP system is always less than that in the MEA system at the same concentration as well as the decreasing ratio of RIAC according to C_{ini} in the AMP system, 0.10 L/mol, was higher than that in the MEA system. The chemical CO_2 absorption capacity required to raise the same electrical conductivity in the AMP solution is larger than that in the MEA at the same concentration. These differences between the two systems can be attributed to their different molecular structures and sizes.

1. INTRODUCTION

Climate change caused by the CO_2 concentration increase in the atmosphere is believed to be one of the most important environmental issues. In order to selectively capture CO_2 emitted from the flue gas generated in coal-fired power plants, cement- and steel-production industries, etc., many carbon capture & storage (CCS) technologies have been investigated and some of them began to be commercialized.[1−6]

One of the representative chemical absorbents to capture CO_2 is alkanolamine-based aqueous solution. In particular, the chemical absorption process using monoethanolamine (MEA) solvent, one of the primary amines, has been commercialized with enhanced oil recovery in the U.S. and Canada.[7−9] MEA reacts directly with CO_2 at a faster reaction rate than that of other amines. Although the MEA utilization increases theoretically to about 1.0 mol CO_2/mol MEA by carbamate ($RNHCOO^-$) hydrolysis in the low-concentration MEA solution or high CO_2 partial pressure, the utilization is generally controlled so as to not exceed 0.5 mol CO_2/mol MEA using a high-concentration MEA solution to prevent the corrosion of the equipment. In addition, the high energy consumption for solvent regeneration needs to be decreased in order to improve the economy of the process.[10,11] Hence, many studies have been carried out to investigate a novel catalyst, new chemical absorbent, and hybrid systems to diminish the presently excessive energy consumption. 2-Amino-2-methyl-1-propanol (AMP), a primary and sterically hindered amine, is considered an attractive absorbent to substitute for MEA because an AMP system can be operated with a high theoretical utilization of 1.0 in high AMP concentrations and as the energy requirements for solvent regeneration are relatively low due to the steric hindrance effect.[12,13] However, the system's slow reaction rate, when using solely AMP alone as a solvent, has prohibited its practical use.[14] Therefore, research has focused on using AMP in blended solvents to increase the performance of the main solvent. Conway et al. proposed the MEA-AMP blended solvent as an alternative to the 5 M-MEA solution, which is currently commercially used,[15] among the various combined AMP systems with MEA, *N*,*N*-dimethylethanolamine (DMEA), and *N*,*N*-diethylethanolamine (DEEA). In addition, much research has reported the physiochemical and thermodynamic properties of AMP such as the corrosion rate, density, viscosity, and regeneration energy in AMP-blended amine solvent, which can substantially contribute to

Received: September 29, 2020
Revised: January 19, 2021
Published: January 28, 2021

https://dx.doi.org/10.1021/acs.energyfuels.0c03283
Energy Fuels 2021, 35, 3197−3207

improve the performance of the absorption system and to develop the better solvent.[16−19] Considering the merit of AMP in terms of the solvent utilization, however, additional studies on the unique and beneficial characteristics of AMP as the CO_2 absorbent, which have not yet reported, are required for the further development of the AMP-incorporated absorption system.

In the present study, the CO_2 absorption performance and electrical properties of the AMP system were investigated, and their correlated equation was proposed to estimate in situ chemical CO_2 absorption capacity by measuring the electrical conductivity (EC) of the solution during CO_2 absorption. In addition, the results were compared to those of the MEA system, which was reported in our previous papers, focusing on their molecular size and structure, as well as the sterically hindered effect of AMP. Especially, the ionic conductivity (IC) of protonated AMP and the real ionic activity coefficient (RIAC) in high-concentration AMP solution were reported as the electrical properties. These results promise to contribute to the optimization of the operation control to increase the absorption performance and provide information to enhance the absorption system.

2. THEORY

2.1. Absorption Mechanism Using Tertiary Amine Aqueous Solution. Before CO_2 absorption, the primary amines (denoted as RNH_2) such as AMP and MEA were dissociated in aqueous solution to generate protonated amine (RNH_3^+) and OH^- via eq 1.

$$RNH_2 + H_2O \rightarrow RNH_3^+ + OH^- \quad (1)$$

Here, R is a functional group of $-C(CH_3)_2CH_2OH$ and $-C_2H_4OH$ for AMP and MEA, respectively. The concentration of RNH_3^+ and OH^- generated resulting from eq 1 can be estimated by the dissociation constant (pK) of AMP and MEA, which is 9.42 and 9.68, respectively.[20,21] The CO_2 absorption mechanism of RNH_2 aqueous solution can be summarized in eqs 2−4.

$$OH^- + CO_2 \rightarrow HCO_3^- \quad (2)$$

$$2RNH_2 + CO_2 \rightarrow RNH_3^+ + RNHCOO^- \quad (3)$$

$$RNHCOO^- + H_2O \rightarrow RNH_2 + HCO_3^- \quad (4)$$

$$RNH_2 + H_2O + CO_2 \rightarrow RNH_3^+ + HCO_3^- \quad (5)$$

When CO_2 is injected for absorption, CO_2 first reacts with OH^- generated by eq 1, and then the primary absorption by RNH_2 occurs via eq 3, which is known as a direct reaction between CO_2 and amine. The reaction mechanism is shown in Figure 1 with their molecular formula.[22]

Thereafter, $RNHCOO^-$ is hydrolyzed by water via eq 4 generating the free amine, as shown in Figure 1, which participates again in eq 3 to additionally absorb CO_2. Therefore, if the hydrolysis reaction favorably occurs, the overall absorption reaction can be expressed as in eq 5. In the MEA system, the hydrolysis reaction is substantially inhibited in the high-concentration MEA concentration with the high CO_2 partial pressure. However, since eq 4 is almost simultaneously carried out with eq 3, even in highly concentrated solutions, due to the steric hindrance effects of AMP, the overall absorption reaction in the AMP system is expressed as in eq 5; hence, the theoretical molar ratio of

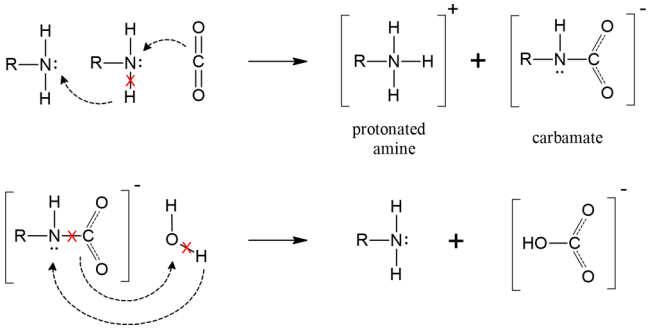

Figure 1. CO_2 absorption mechanism using primary amine (AMP and MEA) solutions.[22]

absorbed CO_2 to AMP molecules in solution is 1.0 mol CO_2/mol AMP. However, when CO_2 was absorbed in very high-concentration AMP solutions, some of the AMP carbamate ($AMPCOO^-$) generated cannot be hydrolyzed but is rather converted the zwitterions and thus the reaction mechanism in this case is expressed as eqs 6 and 7.[23,24]

$$AMPH^+ + AMPCOO^- \leftrightarrow AMPH^+{\cdot}AMPCOO^-_{(aq)} \quad (6)$$

$$AMPH^+{\cdot}AMPCOO^-_{(aq)} \rightarrow AMPH{\cdot}AMPCOO_{(s)} \quad (7)$$

As the concentration of zwitterions ($AMPH^+{\cdot}AMPCOO^-$) generated via eq 6 increases, it can be precipitated via eq 7, as was observed in the present work in the absorption with the solutions of containing an AMP concentration above 3.0 M at 25 °C and a CO_2 partial pressure of 0.33 atm, which is a CO_2 concentration in the simulated gas of the cement and steel industry.

2.2. Calculation of Electrical Conductivity (EC). The equation to calculate the electrical conductivity (EC) of the solution is expressed in eq 8.[25,26]

$$EC(S/m) = k_o\gamma^2 \quad (8)$$

Here, k_o (S/m) is the EC of an infinitely diluted solution and γ is the ionic activity coefficient (IAC). First, the k_o value can be calculated via eq 9.

$$k_o(S/m) = \sum z_i\lambda_i c_i \quad (9)$$

where z_i is the absolute value of electric charge of ion i, λ_i is the ionic conductivity of ion i (IC; $S{\cdot}m^2/(mol{\cdot}z)$), c_i is the ionic concentration of ion i (mol/m^3) in the solution, and i represents OH^-, HCO_3^-, $AMPH^+$, $MEAH^+$, and $MEACOO^-$.

For this calculation of k_o, it is assumed that no interactions are exerted between ions and molecules in the solution. However, as the interaction is present in the real solution, IAC is used to compensate for the deviation between the assumed and practical values. IAC is dependent on the ionic strength (IS; mol/L) in solutions as listed in eq 10, and finally, IAC is calculated by the Debye−Huckel, Gutenberg, and Davies equations, respectively, according to the IS range, as represented in eqs 11−13.[27−29]

$$IS(mol/L) = 5 \times 10^{-4} \sum c_i z_i^2 \quad (10)$$

$$\log\gamma = -0.509 z_+ z_- \sqrt{IS} \quad IS < 0.01 \quad (11)$$

$$\log\gamma = -0.5 z_+ z_- \frac{\sqrt{IS}}{1+\sqrt{IS}} \quad 0.01 \le IS \le 0.1 \quad (12)$$

https://dx.doi.org/10.1021/acs.energyfuels.0c03283
Energy Fuels 2021, 35, 3197−3207

Table 1. AMP and MEA Solutions Used in the Absorption with the Initial Molar Concentration (C_{ini}), their Corresponding Mass Concentrations, and the Role of the Solutions Used

classified concentration range	AMP C_{ini} (mol/L)	AMP mass concentration (wt%)	MEA C_{ini} (mol/L)	MEA mass concentration (wt%)	role of solutions in CO_2 absorption
low concentration	0.1	0.9	0.1	0.6	to estimate ionic conductivity of protonated amine and carbamate in each amine system
	0.2	1.8	0.2	1.2	
	0.3	2.7	0.3	1.8	
	0.4	3.6	0.4	2.4	
	0.5	4.5	0.5	3.1	
high concentration	1.0	9.0	1.0	6.1	to estimate real ionic activity coefficient in each amine system
	2.0	18.1	2.0	12.2	
	3.0	27.3	3.0	18.3	
	4.0	36.6	4.0	24.4	
			5.0	30.4	

$$\log \gamma = -0.5 z_+ z_- \left(\frac{\sqrt{IS}}{1 + \sqrt{IS}} - 0.2IS \right) \quad 0.1 < IS < 0.5 \tag{13}$$

Therefore, the three values (ionic concentration, IC, and electric charge) are required to calculate the EC of the solutions. However, when the IS of solution is higher than 0.5 M, since none of eqs 11−13 could be employed, the other equation as expressed in eq 14 is necessarily required to calculate RIAC (γ_c) instead of IAC.

$$\gamma_c = \sqrt{\frac{EC_m}{k_o}} \quad \text{In high} - \text{concentration amine solution} \tag{14}$$

Equation 14 is a modified version of eq 8 by substituting EC and IAC with EC measured (EC_m) and RIAC in the solution, respectively. In the present paper, RIAC was calculated by eq 14 with EC_m when the IS of amine solution is higher than 0.5 M.

3. EXPERIMENTAL PROCEDURE

AMP and MEA solutions used in the absorption are summarized in Table 1 with the molar concentration and their corresponding mass concentrations (wt %).

For convenience, the solutions were classified into the low- and high-concentration solutions according to the initial molar concentration of amine in solutions (C_{ini}). Their concentration ranges and their specific applications in the absorption are detailed in Table 2. In addition, the absorption performance and electrical properties of the AMP and MEA systems were compared in all the two concentration-ranged solutions. A schematic diagram of the absorption experiment is shown in Figure 2.

Table 2. Ionic Conductivity (IC) and Minimum Calculation Deviation of the Ions Generated

ions	ionic conductivity ($S \cdot cm^2/(mol \cdot z)$)	calculation deviation (%)
OH^-	198.6	
HCO_3^-	44.5	
$AMPH^+$	29.1[a]	7.49
$MEAH^+$	62.2[b]	3.85
$MEACOO^-$	25.4[b]	4.42

[a]Calculated value in the present work. [b]Calculated value in the previous work.[34]

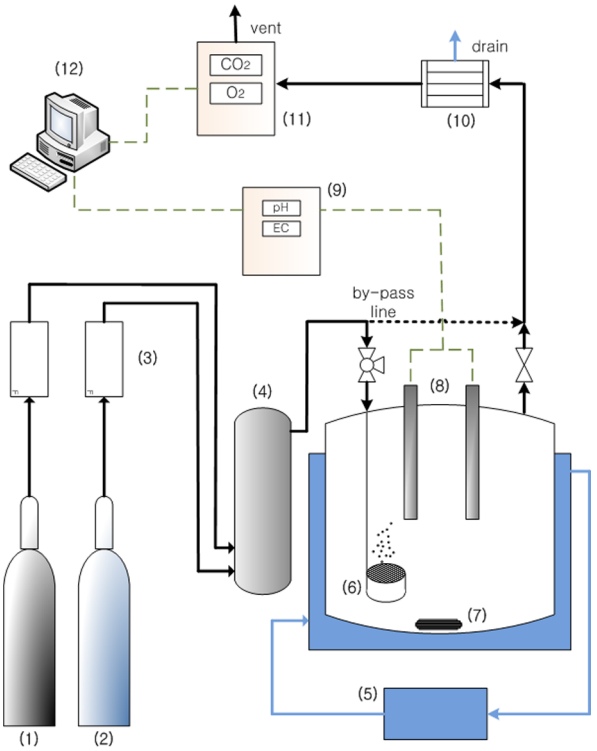

Figure 2. Schematic diagram of CO_2 absorption using the AMP and MEA solutions: (1) N_2 cylinder, (2) CO_2 cylinder, (3) mass flow controller (MFC), (4) gas mixer, (5) water circulator, (6) sparger, (7) magnetic stirrer, (8) pH/EC meter, (9) pH/EC recorder, (10) condenser, (11) gas analyzer, and (12) computer for data acquisition.

For absorption, 500 mL of the 11 AMP and MEA solutions (Table 1) were placed in a cylindrical reactor (D, 110 mm; h, 80 mm; total volume, 760 cm^3) equipped with a water jacket to maintain a constant temperature of 25 °C. The solutions were uniformly mixed using a magnetic bar at a constant speed of 180 rpm. Before the absorption, all of the empty spaces in the apparatus, including the reactor, were cleaned by purging with pure N_2 gas. The CO_2 (99.9%) and N_2 (99%) gases are uniformly mixed in an SUS-made gas mixer (*D*, 90 mm; *h*, 400 mm; total volume, 2545 cm^3) with their flow rates of 2 and 1 L/min, respectively, using a mass flow controller (MFC; MPR-200, MKP) in preparation for absorption. Before the absorption, the concentration of CO_2 in the gas mixture was confirmed to be 33.3 vol % using a nondispersive infrared (NDIR) CO_2 gas analyzer (GA; maMos-200, Madur Electronics). The absorption was conducted by injecting the gas mixture into the reactor through a 1 μm pore-sized

https://dx.doi.org/10.1021/acs.energyfuels.0c03283
Energy Fuels 2021, 35, 3197−3207

sparger for a uniformly dispersed reaction in the solution. The gas mixture passed through the reactor for absorption and exited from the reactor to the GA to measure the CO_2 concentration in the gases. The flow rate of the outlet gas into the GA was maintained as 1.5 L/min by a sampling pump and the humidity in the outlet gases was eliminated by a condenser maintained at 1 °C before injection into the GA. The CO_2 concentration of the outlet gas was measured every 1 s during the absorption, while the pH and EC of the solution were measured every 5 s using a pH/EC meter (Orion 4 Star, Thermo Scientific). The standard uncertainty (u) of experimental data is $u(C_{ini})$ = 0.001 mol/L, $u(c_{CO2})$ = 0.01%, $u(P)$ = 0.01 MPa, $u(T)$ = 1.0 K, and u(EC) = 0.05 μS/cm. Here, P and T are pressure and temperature, respectively. All the measured data were automatically recorded and treated using data acquisition systems.

4. RESULTS AND DISCUSSION

4.1. Chemical CO_2 Absorption Capacity and Amine Utilization. The experimentally measured chemical CO_2 absorption capacity (mol CO_2/L of solution; CAC_{chem}) according to C_{ini} is shown in Figure 3 with the theoretical

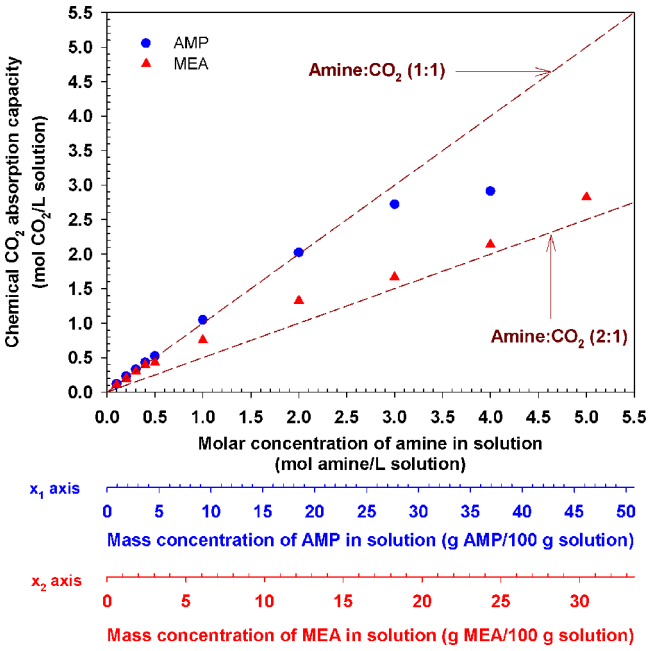

Figure 3. Experimental and theoretical chemical CO_2 absorption capacities according to the initial molar (and mass) concentration of amine in the AMP and MEA solutions.

values calculated based on eqs 3 and 5. In addition, the mass concentrations of AMP and MEA, which correspond to their C_{ini}, were added to the bottom of the X-axis as x_1- and x_2-axes to readily compare how their mass concentrations are quantitatively different at the same molar concentration. CAC_{chem} is the amount of chemically absorbed CO_2 divided by the volume of the solutions, and it is determined by subtracting the amount of physically absorbed CO_2 from the total amount of absorbed CO_2 measured by the GA during the absorption. Here, the amount of physically absorbed CO_2 in the solutions was estimated based on the total amount of absorbed CO_2 in pure water and on the water concentration in the AMP and MEA aqueous solutions. The methodology for calculating the total amount of absorbed CO_2 was detailed in our previous paper.[30]

The CAC_{chem} of the AMP solutions below 2.0 M was similar to the theoretical value based on 1:1 (mol amine:mol CO_2) reaction (eq 5). However, CAC_{chem} from the solutions with higher concentration than 2.0 M decreased below the theoretical value of the 1:1 reaction, down to 2.91 mol CO_2/L of solution in the 4.0 M solutions, which is 27.3% less than the theoretical value. CAC_{chem} in the MEA system was close to the theoretical line in the solution below 0.4 M. However, it was gradually decreased below the theoretical value from the 0.5 M solution and the difference became larger than the theoretical value according to C_{ini} to be 2.14 mol CO_2/L of solution in the 4.0 M MEA solution, which is similar to the theoretical value obtained for the 2:1 reaction. From the results, while the 1:1 reaction (eq 5)) may have been dominant below 0.4 M in the MEA system but then gradually shifted to a 2:1 reaction as C_{ini} increased, the reaction may have primarily occurred even in the relatively high-concentration AMP solution of 2.0 M. The results of the MEA system are attributed to the inhibition of the hydrolysis of MEA carbamate ($MEACOO^-$) by the decreased water concentration as C_{ini} increases in the solutions. However, in the AMP system, the concentration required to shift the 1:1 reaction to 2:1 reaction was five times higher than that of the MEA system. This is attributed to the relatively higher instability due to the steric hindrance effect of AMP, which will be detailed in the next section.

The portion of $RNHCOO^-$ participating in the hydrolysis reaction of eq 4 among the total $RNHCOO^-$ generated, i.e., the hydrolysis ratio of $AMPCOO^-$ and $MEACOO^-$, is shown in Figure 4. The amounts of hydrolyzed and generated $RNHCOO^-$ were stoichiometrically calculated using CAC_{chem} measured in each solution, assuming that eqs 3 and 4 occurred consecutively.

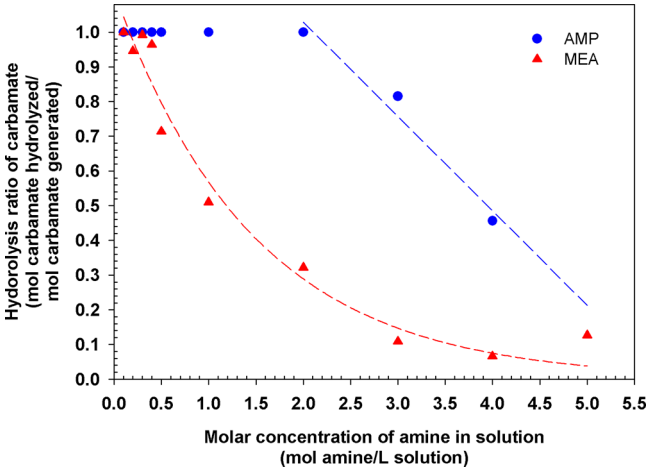

Figure 4. Hydrolysis ratio of carbamate and these regression results according to the initial molar concentration of amine in the AMP and MEA solutions.

The $RNHCOO^-$ generated from the absorption was almost completely hydrolyzed in the AMP and MEA solutions below 2.0 and 0.4 M, respectively. In the higher concentration solutions, the hydrolysis ratio gradually decreased according to C_{ini}, and thus, the ratio was 45.6% in 4.0 M AMP, which was much higher than 6.6% of 4.0 M MEA. This result in the solutions below 2.0 M AMP and 0.4 M MEA is basically attributed to the presence of sufficient water molecules around $RNHCOO^-$ for hydrolysis in those solutions. However, although the ratio of the water molecules to $RNHCOO^-$ in

https://dx.doi.org/10.1021/acs.energyfuels.0c03283
Energy Fuels 2021, 35, 3197−3207

the 2.0 M AMP solution was 16.7% less than that in the 0.4 M MEA solution, the hydrolysis ratio was higher in the AMP solution than that in the MEA solution. This result is tentatively attributed to the very high instability of $AMPCOO^-$ caused by the large steric hindrance effect of two $-CH_3$ moieties in the AMP molecules.

The stability constants (K_c) of $AMPCOO^-$ and $MEACOO^-$ are 0.28 and 26.77 L/mol, respectively,[31] indicating that it is more difficult for $AMPCOO^-$ to present in the ionic state in the solution, compared to $MEACOO^-$. That is, $AMPCOO^-$ is relatively more basic due to its steric hindrance effect and is therefore more easily hydrolyzed with water and combined with protonated amine, even in relatively high-concentration solution.

The hydrolysis ratio (mol $RNHCOO^-$ hydrolyzed/mol $RNHCOO^-$ generated) in the AMP and MEA solutions according to C_{ini} above 2.0 and 0.4 M, respectively, was correlated and they are depicted as the dotted line in Figure 4 and the correlated equations are expressed in eqs 15 and 16.

$$\text{Hydrolysis ratio of } AMPCOO^-(\text{mol } AMPCOO^- \text{ hydrolyzed/mol } AMPCOO^- \text{ generated}) = -0.27 \cdot C_{ini} + 1.57 \quad C_{ini} > 2.0 \text{ M}, r^2 = 0.97 \tag{15}$$

$$\text{Hydrolysis ratio of } MEACOO^-(\text{mol } MEACOO^- \text{ hydrolyzed/mol } MEACOO^- \text{ generated}) = 1.12 \cdot e^{-0.68 C_{ini}} \quad C_{ini} > 0.4 \text{ M}, r^2 = 0.97 \tag{16}$$

When the absorption was conducted with the 4.0 M AMP and MEA solutions, the amount of $AMPCOO^-$ and $MEACOO^-$ generated via eq 3 was 2.0 M in each solution. Thereafter, they were hydrolyzed by eq 4 and, considering eqs 15 and 16, the hydrolysis ratio of $AMPCOO^-$ and $MEACOO^-$ was calculated to be 48.5 and 7.5%, respectively. Therefore, the concentrations of hydrolyzed $AMPCOO^-$ and $MEACOO^-$ become 0.97 and 0.15 M, and thus the concentrations of the remaining $AMPCOO^-$ and $MEACOO^-$ were 1.03 and 1.85 M in the absorption completed solutions, respectively. Here, while all $MEACOO^-$ molecules were still maintained as the ionic state in the solution, 1.03 M of $AMPCOO^-$ was combined with $AMPH^+$ by eq 6 to generate $AMPH^+ \cdot AMPCOO^-$ as an aqueous state, some of which was precipitated by eq 7.

4.2. Absorption Completion Time (ACT) and Overall Absorption Rate of CO_2 (OAR). The absorption completion time (ACT) and overall absorption rate of CO_2 (OAR) according to C_{ini} in the two systems are shown in Figure 5a,b; the OAR implies the moles of CO_2 absorbed (reacted) per unit time and volume of solution.

ACT increased proportionally to C_{ini} in the AMP system as measured about 247.4 min at the 4.0 M AMP solution. Especially, the increasing ratio of the solutions above 0.5 M was slightly larger than that of the lower concentration solutions. In the MEA system, however, although ACT increased according to C_{ini}, it rapidly increased until 50.7 min in the 0.5 M solutions, and thereafter, the increasing ratio significantly decreased to about 93.4 min in the 5.0 M MEA solution. The different increasing ratios of ACT between the low- and high- concentration solutions is due to shift from the dominant reaction of eq 5 in the low-concentration range to the reaction of eq 3, which occurs relatively slowly in the high-concentration range. On the other hand, the ACT in the AMP solutions increased proportionally to the AMP concentration over the full C_{ini} range because eq 5 occurs solely for absorption, which practically resulted from the instability of AMPCOO- to be rapidly hydrolyzed by eq 4.

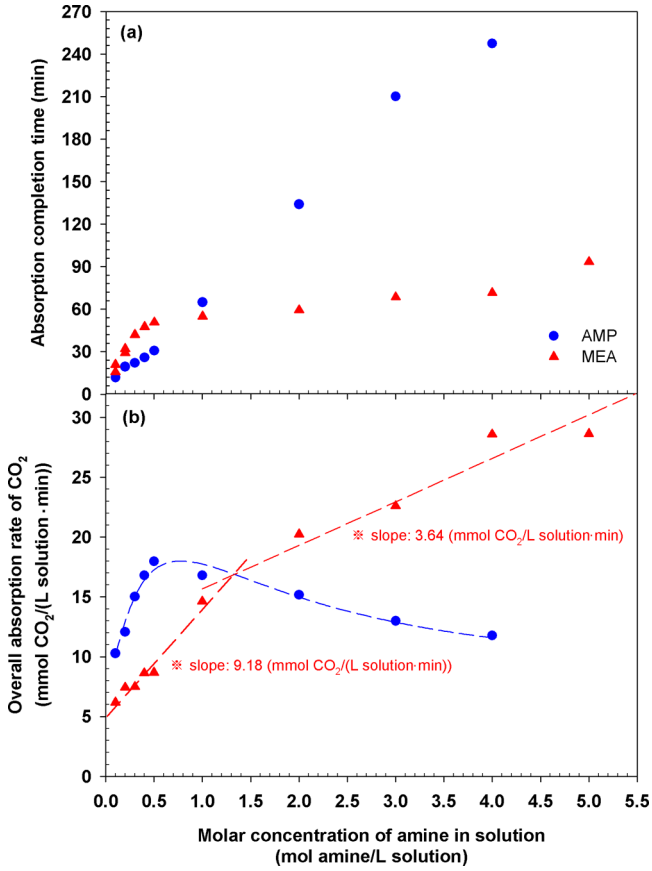

Figure 5. (a) Absorption completion time and (b) overall absorption rate of CO_2 according to the initial molar concentration of amine in the AMP and MEA solutions.

The OAR of the two systems was determined dividing CAC_{chem} (Figure 3) by ACT (Figure 5a) and is shown in Figure 5b. In the MEA system, the increasing ratio of OAR according to C_{ini}, i.e., the slope, differed in the low- and high-concentration ranges at 9.18 and 3.64 mmol CO_2/(mol amine·min), respectively. This can be explained by the reaction order of eq 5, which is the net reaction of eqs 3 and 4, being higher than that of eq 3. On the other hand, the variation of OAR in the AMP system followed a parabolic curve, such as for a single base-catalytic reaction that is generally observed in the absorption with tertiary amine solvents such as TEA and MDEA.[32] The OAR gradually decreased according to C_{ini} from a maximum of 17.98 mmol CO_2/(L·min) in the 0.5 M AMP solution to 11.77 mmol CO_2/(L·min) in the 4.0 M solution.

The OAR in the low-concentration range in the AMP system was significantly larger than that in the MEA system because $AMPCOO^-$ was consumed even faster than $MEACOO^-$ by eq 4. In the high-concentration range, OAR was decreased according to the AMP concentration because the amount of generated free-AMP was reduced in this range due to the low hydrolysis ratio of $AMPCOO^-$, and some of $AMPCOO^-$ were combined with the generated $AMPH^+$ via eqs 6 and 7 to be aqueous and solid AMPCOO·AMPH, which might inhibit the CO_2 absorption.

https://dx.doi.org/10.1021/acs.energyfuels.0c03283
Energy Fuels 2021, 35, 3197−3207

4.3. Ionic Conductivity (IC) of Protonated Amine and Carbamate in the AMP and MEA Systems. The IC of $AMPH^+$, $MEAH^+$, and $MEACOO^-$ calculated based on EC and the ionic concentrations measured in the solution of the low-concentration range are summarized in Table 2 with their calculation deviations and the generally reported IC values of OH^- and HCO_3^-.[33]

The IC of $AMPH^+$ was calculated via eqs 8−14, and the factors required for the calculation are the ICs and electric charges of OH^- and HCO_3^-, as well as the EC of the solutions. Here, EC was used as EC_m measured during the absorption, and the ionic concentration was calculated as follows. First, the concentrations of $AMPH^+$, $MEAH^+$, and OH^- in the initial solutions before absorption were calculated via the dissociation constants (pK_a) of AMP and MEA, which are 9.70 and 9.42, respectively.[20,21] Second, when CO_2 was injected into the solutions, CO_2 was first absorbed by OH^- to generate HCO_3^- via eq 2. Thereafter, absorption mainly resulted from amine according to eq 3, followed by eq 4. However, although AMP was the primary amine, the absorption reaction appeared to be represented by eq 5 due to the steric hindrance effect. Therefore, the ionic concentrations in the low-concentration AMP solution was stoichiometrically calculated using eq 5 with CAC_{chem} measured every second during the absorption. As a result, the IC of $AMPH^+$ was determined as 29.1 $S{\cdot}cm^2/(mol{\cdot}z)$ with a minimum calculation deviation of 7.49%. The ICs of $MEAH^+$ and $MEACOO^-$ have been reported to be 62.2 and 25.4 $S{\cdot}cm^2/(mol{\cdot}z)$ with minimum calculation deviations of 3.85 and 4.42%, respectively, and the calculation process was detailed in our previous work.[34]

The IC of $AMPH^+$ was 46.8% less than that of $MEAH^+$, which can be significantly attributed to their different molecular weights and partial molar volumes. The mobility of ion, which is directly related to IC, is inversely proportional to the molecular weight and to the partial molar volume.[35] Since the molecular weights of $AMPH^+$ and $MEAH^+$ are 90.14 and 62.08 g/mol and the partial molar volumes of AMP and MEA are 89.6 and 59.2 cm^3/mol, respectively,[36,37] the mobility of $AMPH^+$ is less than that of $MEAH^+$, resulting in the lower IC of $AMPH^+$. In addition, the positive charge of the hydrogen ion bound to the N atom in $AMPH^+$ may have been diminished due to the steric hindrance effect, which further decreased the IC of $AMPH^+$.

4.4. Comparison of Measured and Calculated Electrical Conductivities (EC) in the AMP and MEA Systems. Figure 6 shows the variation of EC_m and EC_c according to the absorption time in the low-concentration ranges of the two systems.

The variation trend of EC_m and EC_c was very similar in all the solutions. EC_m increased rapidly during the initial absorption time, but then its increasing ratio gradually reduced to the absorption completion point in both systems because the amine concentration was high at the initial absorption time but subsequently was reduced. However, in the MEA system, the increasing ratios of EC_m of the solutions according to the time decreased rapidly at a certain time between 2 and 5 min, as indicated by the short vertical bar in Figure 6b. These results, first, were explained by the fact that the EC_m in the AMP system is solely dependent on the concentration of $AMPH^+$ and HCO_3^- generated from eq 5, which is regarded as an apparently single reaction occurring throughout the absorption. Additionally, CO_2 was initially absorbed in the MEA system via eq 3 until a certain point, after which the

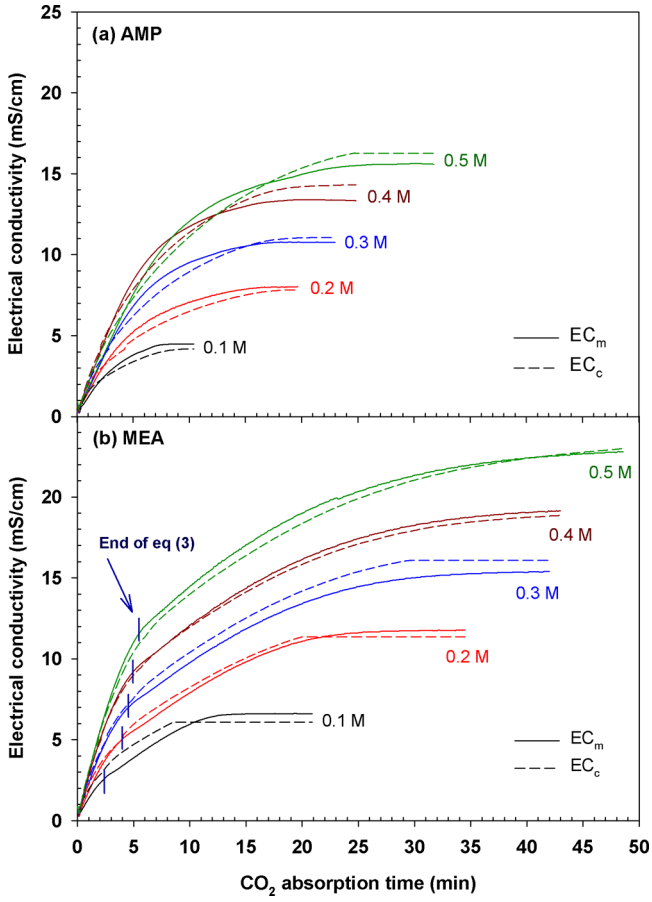

Figure 6. Variations in measured (EC_m) and calculated electrical conductivity (EC_c) according to absorption time in the 0.1−0.5 M (a) AMP and (b) MEA solutions.

progression of eq 4 caused the additional absorption by free-MEA and the reactions were finalized via eq 5. These results implied that the ions present in the MEA solution and their concentrations after the certain time point were very different from those in the AMP solution.

4.5. Real Ionic Activity Coefficient (RIAC) in High-Concentration AMP and MEA Solutions. The RIAC in the high-concentration AMP and MEA solutions saturated with CO_2 (at the absorption completion point) according to C_{ini} and their regression line are shown in Figure 7.

RIAC decreased linearly according to C_{ini} in the high-concentration ranges of the two systems because the interaction between the ions in the solution was stronger due to the high concentration of amine. The RIAC values of 4.0 M AMP and MEA solutions were 0.26 and 0.48, respectively, and the RIAC of AMP solution was always smaller than that of the MEA system at the same concentrations. In addition, the decreasing ratio of RIAC according to C_{ini} in the AMP system (0.10 L/mol) was higher than that in the MEA system (0.06 L/mol) because of the different species of ions present in the two solutions and their different sizes. Although the AMP molecule is very similar to MEA in terms of molecular structure, it is larger than the MEA molecule (or ions) due to the large 2-methyl-1-propanol moiety attached to the N atom in AMP instead of the hydroxyethyl moiety in MEA. Therefore, at the same concentrations of the two systems, the molecules (or ions) in the AMP solutions were relatively closer and their

https://dx.doi.org/10.1021/acs.energyfuels.0c03283
Energy Fuels 2021, 35, 3197−3207

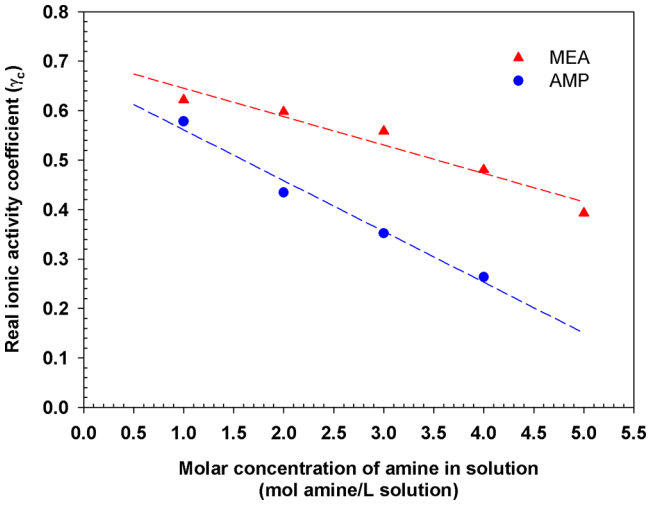

Figure 7. Real ionic activity coefficient (RIAC) in the high-concentration (above 1.0 M) AMP and MEA solutions (γ_c) saturated with CO_2 and their regression results.

interactions were further intensified, which decreased RIAC in the AMP system. RIAC was further decreased due to the steric hindrance effect in the AMP system, i.e., the concentration of effective AMPCOO- was decreased since they were reacted with $AMPH^+$ by eqs 6 and 7 to be stabilized. Thus, although the CAC_{chem} of the AMP system was higher than that of the MEA system in the high-concentration AMP solution, the portion of ions available to increase RIAC in the AMP solutions was reduced due to their higher concentration. In addition, the instability of $AMPCOO^-$ is another significant factor that lowered the RIAC of AMP more than that of the MEA system at the same concentration.

4.6. Correlation between Chemical CO_2 Absorption Capacity (CAC_{chem}) and Electrical Conductivity (EC) in High-Concentration AMP and MEA Solutions. The variations of CAC_{chem} and EC_m according to the absorption time in the high-concentration solutions of the two systems are shown in Figure 8.

Overall, the CAC_{chem} and EC_m variations of the constant concentration solutions increased according to the absorption time with a similar pattern in the two systems. However, although the CAC_{chem} at the completion point in the AMP and MEA solutions increased proportionally to C_{ini} as shown in Figure 8a,c, EC_m was not subjected to C_{ini}, as shown in Figure 8b,d, in the two systems. For example, the EC_m of the 2.0 M AMP and 3.0 M MEA solutions saturated with CO_2 was larger than that of their higher concentration solutions, which indicates that the decrease of RIAC due to the high concentration of amine was further intensified in the two solutions higher than 2.0 M AMP and 3.0 M MEA. Nevertheless, the variation of CAC_{chem} and EC_m according to absorption time for a constant concentration solution was similar in the two systems. That is, CAC_{chem} and EC_m increased rapidly in the initial absorption period, but then their increasing ratio decreased as the absorption approached the completion point. This similarity is because CAC_{chem} is directly related to the ions present in the solutions and their concentration, which are also proportional to EC_m. Therefore, CAC_{chem} is directly proportional to EC_m for a constant concentration solution. Figure 9 shows the correlation between CAC_{chem} and EC_m at the same time during the absorption.

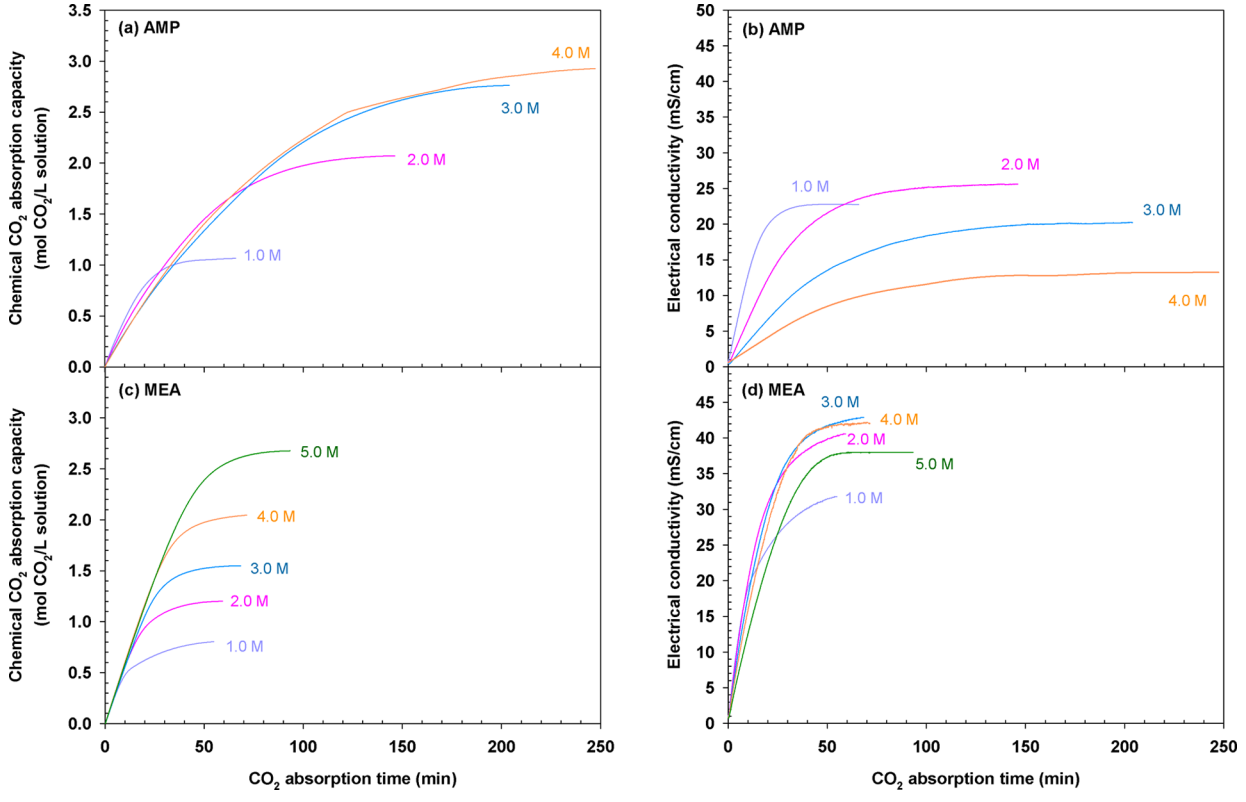

Figure 8. Chemical CO_2 absorption capacity and measured electrical conductivity (EC_m) according to absorption time in the (a, b) AMP and (c, d) MEA solutions.

https://dx.doi.org/10.1021/acs.energyfuels.0c03283
Energy Fuels 2021, 35, 3197−3207

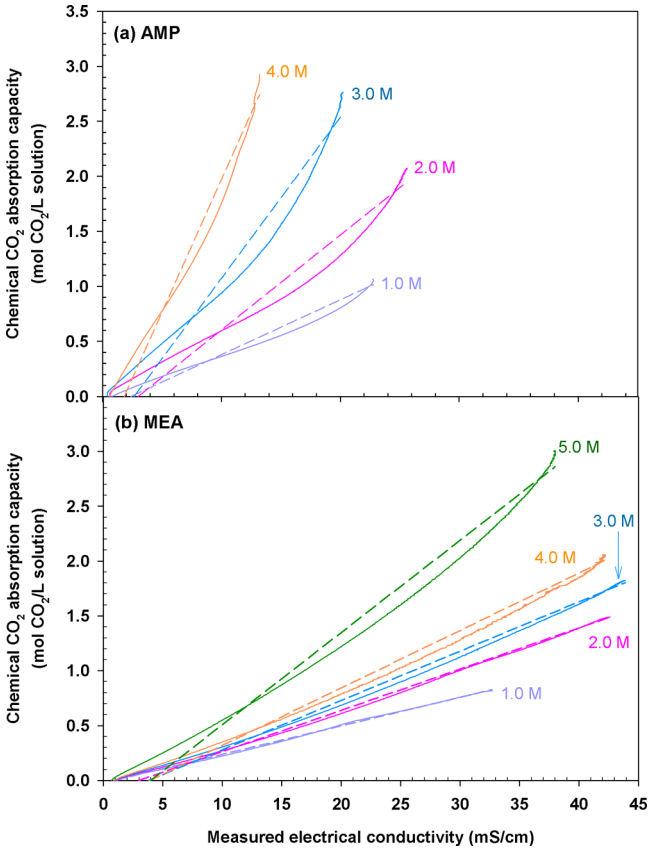

Figure 9. Correlation between the chemical CO_2 absorption capacity and the measured electrical conductivity (EC_m) and their regression results in the (a) AMP and (b) MEA solutions.

All the regression coefficients (r^2) in the two systems were higher than 0.96, and thus it was acceptable to express the linearity between CAC_{chem} and EC_m as a first-order equation in the two systems.[38,39] The slope of CAC_{chem} to EC_m gradually increased as C_{ini} increased; i.e., the amount of CAC_{chem} required to raise the constant EC during the absorption increased as C_{ini} increased. For example, CAC_{chem} required to increase 10 mS/cm of EC in the 2.0 and 4.0 M AMP solutions was 0.59 and 1.75 mol CO_2/L, respectively; i.e., about three times more CAC_{chem} was required to increase a unit EC in the 4.0 M AMP solution than in the 2.0 M AMP solution. This is because RIAC was further decreased as C_{ini} increased in the solution, so that more CAC_{chem} was required in the high-concentration solution to generate as much as the concentrations of effective ions to increase the same EC in the low-concentration solution. In the MEA system, the CAC_{chem} values required to increase 10 mS/cm of EC in the 2.0 and 4.0 M solutions were 0.27 and 0.35 mol CO_2/L, respectively, which are relatively less than those in the AMP system because of the relatively higher RIAC and IC of the ions in the MEA system. The correlations between CAC_{chem} and ECm in the two systems shown in Figure 9 can be generalized as listed in eq 17.

$$CAC_{chem}(\text{mol } CO_2/\text{L of solution}) = a\cdot(EC_m \text{ of solution}) + b \quad (17)$$

where a is the slope of CAC_{chem} to ECm in the correlated equation (SCE) and b is the y-intercept (ICE).

SCE and ICE were dependent on C_{ini} and their values are shown in Figure 10.

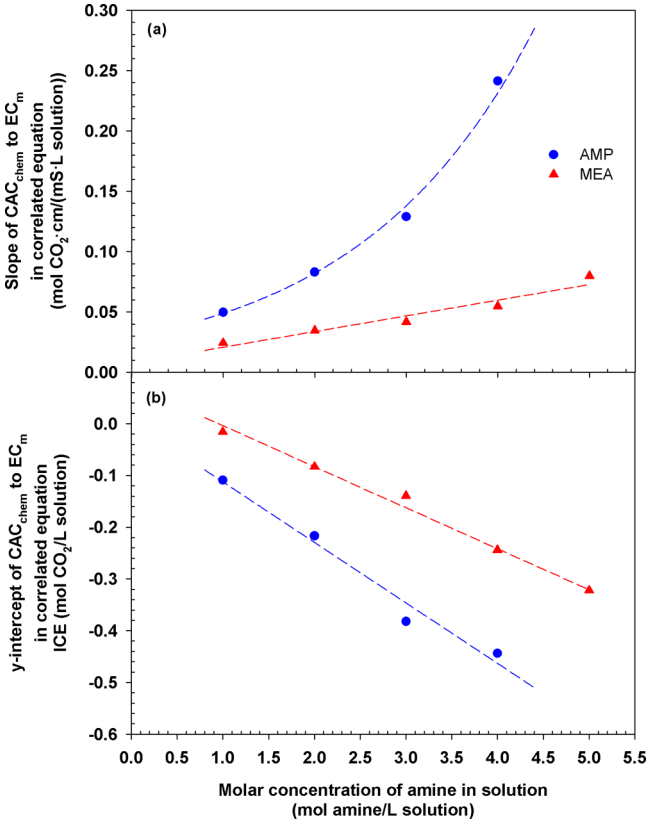

Figure 10. Variation of the (a) slope (SCE) and (b) y-intercept (ICE) in the correlated equation between the chemical CO_2 absorption capacity and the measured electrical conductivity (EC_m) according to the initial molar concentration of amine in the AMP and MEA solutions.

While SCE in the AMP system was increased with an exponential function, SCE in the MEA system was linearly increased according to C_{ini}. This difference implied that CAC_{chem} required to raise the constant EC in the AMP system is larger than that in the MEA system because the concentration of effective ions that affect the SCE of the solution was relatively smaller in the AMP solution and as the IC of $AMPH^+$ was less than half that of $MEAH^+$. Here, the concentration of effective ions was determined as the product of concentrations of total ions and the squared IAC of the solution. For example, the concentrations of total $AMPCOO^-$ and $MEACOO^-$ of the 4.0 M solution were 2.91 and 2.14 M at their absorption completion points, respectively, and IAC^2 was 0.07 for 4.0 M AMP and 0.23 for 4.0 M MEA solutions. Therefore, the concentration of effective $AMPCOO^-$ of the 4.0 M AMP solution was 0.20 M, which is smaller than the equivalent value of 0.49 M of the 4.0 M MEA solution. In addition, as aforementioned, HCO_3^- and $MEACOO^-$ are theoretically generated to the extent of the concentrations of $AMPH^+$ and $MEAH^+$ produced by eqs 5 and 3, as their conjugate anions, in the AMP and MEA systems, respectively. Here, the IC of HCO_3^- is higher than that of $MEACOO^-$. However, since the sum of IC of $AMPH^+$ and HCO_3^- is less than that of $MEAH^+$ and $MEACOO^-$ and as the concentrations of effective $AMPH^+$ and HCO_3^- are less than

https://dx.doi.org/10.1021/acs.energyfuels.0c03283
Energy Fuels 2021, 35, 3197−3207

those of $MEAH^+$ and $MEACOO^-$, the SCE of the AMP system is relatively higher than that of the MEA system at the same concentration.

ICE decreased proportionally to C_{ini} in the two systems, as shown in Figure 10b. ICE indicates CAC_{chem} when EC_m is zero in the solution. However, although CAC_{chem} is zero, the solution always shows a certain value of EC. Therefore, ICE is an only mathematical factor necessary for the equation derivation. As a result, the correlations between SCE and C_{ini} and between ICE and C_{ini} in the two systems can be expressed in eqs 18−21.

$$\text{SCE of AMP} = e^{0.518}\cdot C + 3.535 \quad r^2 \text{ is } 0.99 \tag{18}$$

$$\text{SCE of MEA} = 0.013\cdot C + 0.008 \quad r^2 \text{ is} 0.94 \tag{19}$$

$$\text{ICE of AMP} = -0.117\cdot C + 0.004 \quad r^2 \text{ is } 0.97 \tag{20}$$

$$\text{ICE of MEA} = -0.079\cdot C + 0.076 \quad r^2 \text{ is } 0.99 \tag{21}$$

Finally, substituting the term in the right-hand side of eqs 18−21 for a and b of eq 17, the correlated equation, which in situ estimates CAC_{chem} by measuring EC during the absorption at the certain C_{ini} in the solutions, is generalized in the AMP and MEA systems as listed in eqs 22 and 23, respectively.

$$\text{CAC of AMP(mol } CO_2/\text{L)} = (e^{0.518C+3.535})\cdot \text{EC} - 0.117\cdot C + 0.004 \tag{22}$$

$$\text{CAC of MEA(mol } CO_2/\text{L)} = (0.013C + 0.008)\cdot EC_m - 0.079\cdot C + 0.076 \tag{23}$$

5. CONCLUSIONS

The present study quantitatively investigated the features of the two CO_2 chemical absorption systems using the primary amine-base absorbents, namely AMP and MEA aqueous solutions, by comparing their absorption performance and electrical properties. The differences between the two systems were mostly attributed to the water concentration in the solutions, molecular structures and size of amine. From the results, the conclusions were derived as follows.

(i) The chemical CO_2 absorption capacity (CAC_{chem}) measured in the solutions with concentrations less than 2.0 M AMP and 0.4 M MEA was very close to its theoretical values (eq 5). However, the CAC_{chem} in the AMP solutions above 2.0 M was reduced below the theoretical values and this decrement increased according to C_{ini} due to the instability of $AMPCOO^-$ caused by the steric hindrance effects in the high-concentration solution. On the other hand, in the MEA solutions above 0.4 M, CAC_{chem} begun to significantly decrease, which indicated that eq 5 was shifted to eq 3 due to the inhibition of the hydrolysis of $MEACOO^-$ resulting from the low water concentration in the solutions. Therefore, the critical concentration of the two solutions necessary to strongly impact the absorption performance was verified to be 2.0 and 0.4 M in the AMP and MEA systems, respectively.

(ii) Unlike the MEA system, the increasing ratio of ACT according to C_{ini} in the AMP system remained almost constant in all the solutions because the absorption occurred solely via eq 5 over the full concentration range. In addition, the variation of OAR in the AMP system followed a parabolic function of C_{ini} with a maximum of 17.98 mmol CO_2/(L·min) in the 0.5 M. OAR in the high-concentration AMP solutions decreased due to the reduced amount of generated free AMP, which was caused by the combination of the generated $AMPH^+$ with $AMPCOO^-$ via eq 6.

(iii) Since the mobility of $AMPH^+$ decreased due to its larger molecular weight and partial molar volume, as well as to the reduced charge intensity of hydrogen in $AMPH^+$ because of the steric hindrance effect, the IC of $AMPH^+$ was 29.1 S·cm^2/(mol·z), which was 53.2% less than that of $MEAH^+$. RIAC in the AMP system was always less than that in the MEA system at the same concentration, and the decreasing ratio of RIAC according to C_{ini} was higher in the AMP system. In addition, the interaction between the molecules (or ions) was further intensified at the same concentration because the AMP molecule is larger than the MEA one and the stability of $AMPCOO^-$ is very low in terms of reactivity.

(iv) The slope of CAC_{chem} to EC_m in the correlated equation (SCE) according to C_{ini} was exponentially and linearly increased in the AMP and MEA systems, respectively. SCE in the AMP system was always higher than that in the MEA system at the same concentration, which implies that the CAC_{chem} required to raise the same EC in the AMP solution was larger than that in the MEA solution. This is because the concentration of effective ions in the AMP system and the IC of $AMPH^+$ were relatively low compared to the MEA system.

These results cannot yet be generalized because only two types of primary amine system were studied. However, the same experimental method can be applied to other primary-type amine-based solution systems to analyze their comparative absorption performance. Finally, the absorption performance of the primary amine-based solution systems is expected to be systematically and qualitatively analyzed via their molecular size and structure with a moiety attached to the N atom.

AUTHOR INFORMATION

Corresponding Author

Jung-Ho Wee − *Department of Environmental Engineering, The Catholic University of Korea 43 Jibong-ro, Bucheon-si 14662, Republic of Korea;* orcid.org/0000-0001-5142-2391; Phone: +82-2-2164-4866; Email: jhwee@catholic.ac.kr, jhwee@korea.ac.kr; Fax: +82-2-2164-4765

Author

Sang-Jun Han − *Department of Environmental Engineering, The Catholic University of Korea 43 Jibong-ro, Bucheon-si 14662, Republic of Korea;* orcid.org/0000-0002-7095-3208

Complete contact information is available at: https://pubs.acs.org/10.1021/acs.energyfuels.0c03283

Notes

The authors declare no competing financial interest.

ACKNOWLEDGMENTS

This research was supported by the Basic Research Program through the National Research Foundation of Korea (NRF) funded by the Ministry of Education

https://dx.doi.org/10.1021/acs.energyfuels.0c03283
Energy Fuels 2021, 35, 3197−3207

(2017R1D1A1B03033107) as well as supported by the Catholic University of Korea, Research Fund, 2019.

REFERENCES

(1) Sun, J.; Liu, W.; Wang, W.; Hu, Y.; Yang, X.; Chen, H.; Zhang, Y.; Li, X.; Xu, M. Optimizing synergy between phosphogypsum disposal and cement plant CO_2 capture by the calcium looping process. *Energy Fuels* **2016**, *30*, 1256−1265.

(2) Baker, R. W.; Freeman, B.; Kniep, J.; Huang, Y. I.; Merkel, T. C. CO_2 Capture from cement plants and steel mills using membranes. *Ind. Eng. Chem. Res.* **2018**, *57*, 15963−15970.

(3) Pan, S. Y.; Chen, Y. H.; Chen, C. D.; Shen, A. L.; Lin, M.; Chiang, P. C. High-gravity carbonation process for enhancing CO_2 fixation and utilization exemplified by the steelmaking industry. *Environ. Sci. Technol.* **2015**, *49*, 12380−12387.

(4) Hong, S.; Sim, G.; Moon, S.; Park, Y. Low-Temperature Regeneration of Amines Integrated with Production of Structure-Controlled Calcium Carbonates for Combined CO_2 Capture and Utilization. *Energy Fuels* **2020**, *34*, 3532−3539.

(5) Beck, L. Carbon capture and storage in the USA: the role of US innovation leadership in climate-technology commercialization. *Clean Energy* **2020**, *4*, 2−11.

(6) Coker, J.; Afari, D. B.; Narku-Tetteh, J.; Idem, R. Mass-transfer studies of solid-base catalyst-aided CO_2 absorption and solid-acid catalyst-aided CO_2 desorption for CO_2 capture in a pilot plant using aqueous solutions of MEA and blends of MEA-MDEA and BEA-AMP. *Clean Energy* **2019**, *3*, 263−277.

(7) Brickett, L.; Munson, R.; Litynski, J. U.S. DOE/NETL large pilot-scale testing of advanced carbon capture technologies. *Fuel* **2020**, *268*, 117169.

(8) Vega, F.; Baena-Moreno, F. M.; Fernández, L. M. G.; Portillo, E.; Navarrete, B.; Zhang, Z. Current status of CO_2 chemical absorption research applied to CCS: Towards full deployment at industrial scale. *Appl. Energy* **2020**, *260*, 114313.

(9) Mantripragada, H. C.; Zhai, H.; Rubin, E. S. Boundary Dam or Petra Nova−Which is a better model for CCS energy supply? *Int. J. Greenh. Gas Control* **2019**, *82*, 59−68.

(10) Kladkaew, N.; Idem, R.; Tontiwachwuthikul, P.; Saiwan, C. Corrosion behavior of carbon steel in the monoethanolamine−H_2O−CO_2−O_2−SO_2 system: products, reaction pathways, and kinetics. *Ind. Eng. Chem. Res.* **2009**, *48*, 10169−10179.

(11) Handojo, L.; Yudiyanto; Prihartoni, M. D.; Susanti, R. F.; Yaswari, Y.; Raksajati, A.; Indarto, A. Non-oxidative thermal degradation of amines: GCMS/FTIR spectra analysis and molecular modeling. *Sep. Sci. Technol.* **2018**, *53*, 2259−2266.

(12) Sakwattanapong, R.; Aroonwilas, A.; Veawab, A. Reaction rate of CO_2 in aqueous MEA-AMP solution: experiment and modeling. *Energy Procedia* **2009**, *1*, 217−224.

(13) Wai, S. K.; Nwaoha, C.; Saiwan, C.; Idem, R.; Supap, T. Absorption heat, solubility, absorption and desorption rates, cyclic capacity, heat duty, and absorption kinetic modeling of AMP−DETA blend for post−combustion CO_2 capture. *Sep. Purif. Technol.* **2018**, *194*, 89−95.

(14) Nwaoha, C.; Saiwan, C.; Supap, T.; Idem, R.; Tontiwachwuthikul, P.; Rongwong, W.; Al-Marri, M. J.; Benamor, A. Carbon dioxide (CO_2) capture performance of aqueous tri-solvent blends containing 2-amino-2-methyl-1-propanol (AMP) and methyldiethanolamine (MDEA) promoted by diethylenetriamine (DETA). *Int. J. Greenh. Gas Control* **2016**, *53*, 292−304.

(15) Conway, W.; Bruggink, S.; Beyad, Y.; Luo, W.; Melián-Cabrera, I.; Puxty, G.; Feron, P. CO_2 absorption into aqueous amine blended solutions containing monoethanolamine (MEA), N, N-dimethylethanolamine (DMEA), N, N-diethylethanolamine (DEEA) and 2-amino-2-methyl-1-propanol (AMP) for post-combustion capture processes. *Chem. Eng. Sci.* **2015**, *126*, 446−454.

(16) Campbell, K. L. S.; Zhao, Y.; Hall, J. J.; Williams, D. R. The effect of CO_2-loaded amine solvents on the corrosion of a carbon steel stripper. *Int. J. Greenh. Gas Control* **2016**, *47*, 376−385.

(17) Nwaoha, C.; Idem, R.; Supap, T.; Saiwan, C.; Tontiwachwuthikul, P.; Rongwong, W.; Al-Marri, M. J.; Benamor, A. Heat duty, heat of absorption, sensible heat and heat of vaporization of 2−Amino−2−Methyl−1−Propanol (AMP), Piperazine (PZ) and Monoethanolamine (MEA) tri−solvent blend for carbon dioxide (CO_2) capture. *Chem. Eng. Sci.* **2017**, *170*, 26−35.

(18) Sun, W. C.; Yong, C. B.; Li, M. H. Kinetics of the absorption of carbon dioxide into mixed aqueous solutions of 2-amino-2-methyl-l-propanol and piperazine. *Chem. Eng. Sci.* **2005**, *60*, 503−516.

(19) Karunarathne, S. S.; Eimer, D. A.; Øi, L. E. Density, viscosity and free energy of activation for viscous flow of CO_2 loaded 2-amino-2-methyl-1-propanol (AMP), monoethanol amine (MEA) and H_2O mixtures. *J. Mol. Liq.* **2020**, *311*, 113286.

(20) van Westrenen, J.; van Haveren, J.; Alblas, F. J.; Hoefnagel, M. A.; Peters, J. A.; van Bekkum, H. The synthesis of polyhydroxycarboxylates. Part 6. N-alkylation of amino compounds by a michael-type addition with maleate. *Recl. Trav. Chim. Pays-Bas* **1990**, *109*, 474−478.

(21) Khalili, F.; Henni, A.; East, A. L. L. pK_a values of some piperazines at (298, 303, 313, and 323) K. *J. Chem. Eng. Data* **2009**, *54*, 2914−2917.

(22) Crooks, J. E.; Donnellan, J. P. Kinetics and mechanism of the reaction between carbon dioxide and amines in aqueous solution. *J. Chem. Soc., Perkin Trans. 2* **1989**, *4*, 331−333.

(23) Jo, E.; Jhon, Y. H.; Choi, S. B.; Shim, J. G.; Kim, J. H.; Lee, J. H.; Lee, I. Y.; Jang, K. R.; Kim, J. Crystal structure and electronic properties of 2-amino-2-methyl-1-propanol (AMP) carbamate. *Chem. Commun.* **2010**, *46*, 9158−9160.

(24) Svensson, H.; Hulteberg, C.; Karlsson, H. T. Precipitation of AMP carbamate in CO_2 absorption process. *Energy Procedia* **2014**, *63*, 750−757.

(25) Corti, H. R., Trevani, L. N., Anderko, A. Transport Properties in High Temperature and Pressure Ionic Solutions. In *Aqueous System at Elevated Temperatures and Pressures: Physical Chemistry in Water, Steam and Hydrothermal Solutions*. Palmer, R., Fernandez, P., Harvey, A., Eds.; Academic Press: San Diego, CA, 2004.

(26) Eaton, A. D., Franson, M. A. H. *Standard Methods for the Examination of Water & Wastewater*. Washington, DC, 2005.

(27) Debye, P.; Hückel, E. De la theorie des electrolytes. I. abaissement du point de congelation et phenomenes associes. *Phys. Z.* **1923**, *24*, 185−206.

(28) Davies, C. W. *Ion Association*. Butterworths, London, 1962.

(29) Stumm, W., Morgan, J. J. *Aquatic Chemistry; an Introduction Emphasizing Chemical Equilibria in Natural Waters*. Wiley, New York, 1970.

(30) Han, S.-J.; Yoo, M.; Kim, D.-W.; Wee, J.-H. Carbon dioxide capture using calcium hydroxide aqueous solution as the absorbent. *Energy Fuels* **2011**, *25*, 3825−3834.

(31) Park, S. H.; Lee, K. B.; Hyun, J. C.; Kim, S. H. Correlation and prediction of the solubility of carbon dioxide in aqueous alkanolamine and mixed alkanolamine solutions. *Ind. Eng. Chem. Res.* **2002**, *41*, 1658−1665.

(32) Han, S. J.; Wee, J. H. Correlation of CO_2 absorption performance and electrical properties in a tri-ethanolamine aqueous solution compared to mono-and di-ethanolamine systems. *Environ. Sci. Pollut. Res.* **2020**, 1−18.

(33) Patnaik, P., *Handbook of environmental analysis: chemical pollutants in air, water, soil, and solid wastes*. Crc Press, 2017, DOI: 10.1201/9781315151946.

(34) Han, S. J.; Wee, J. H. Estimation of correlation between electrical conductivity and CO_2 absorption in a monoethanolamine solvent system. *J. Chem. Eng. Data* **2013**, *58*, 2381−2388.

(35) Slattery, J. M.; Daguenet, C.; Dyson, P. J.; Schubert, T. J. S.; Krossing, I. How to predict the physical properties of ionic liquids: a volume-based approach. *Am. Ethnol.* **2007**, *119*, 5480−5484.

(36) Henni, A.; Hromek, J. J.; Tontiwachwuthikul, P.; Chakma, A. Volumetric properties and viscosities for aqueous AMP solutions from 25 C to 70 °C. *J. Chem. Eng. Data* **2003**, *48*, 551−556.

https://dx.doi.org/10.1021/acs.energyfuels.0c03283
Energy Fuels 2021, 35, 3197−3207

(37) Maham, Y.; Teng, T. T.; Hepler, L. G.; Mather, A. E. Densities, excess molar volumes, and partial molar volumes for binary mixtures of water with monoethanolamine, diethanolamine, and triethanolamine from 25 to 80 °C. *J. Solution Chem.* **1994**, *23*, 195−205.
(38) Cicchetti, D. V. Guidelines, criteria, and rules of thumb for evaluating normed and standardized assessment instruments in psychology. *Psychol. Assess.* **1994**, *6*, 284.
(39) Rosner, B. *Fundamentals of biostatistics*. Nelson Education; 2015.

https://dx.doi.org/10.1021/acs.energyfuels.0c03283
Energy Fuels 2021, 35, 3197−3207